Alkene Complexes of Divalent and Trivalent Ruthenium Stabilized by Chelation. Dependence of Coordinated Alkene Orientation on Metal Oxidation State

Martin A. Bennett,* Graham A. Heath, David C. R. Hockless, Ivan Kovacik, and Anthony C. Willis

Contribution from the Research School of Chemistry, The Australian National University, Box 414, Canberra ACT 2601, Australia

Received September 18, 1997

Abstract: Zinc amalgam reduction of tris(acetylacetonato)ruthenium(III), [Ru(acac)$_3$], in the presence of the chelating olefinic N- and O-donor ligands (LL′) 2-vinyl-*N*,*N*-dimethylaniline, *o*-$CH_2{=}CHC_6H_4NMe_2$ (**1**), 2-isopropenyl-*N*,*N*-dimethylaniline, *o*-$CH_2{=}C(CH_3)C_6H_4NMe_2$ (**2**), 3-butenyldimethylamine, $CH_2{=}CHCH_2CH_2NMe_2$ (**3**), 2-allylpyridine, $CH_2{=}CHCH_2C_5H_4N$ (**4**), isomesityl oxide (4-methyl-4-penten-2-one), $CH_2{=}C(CH_3)CH_2COCH_3$ (**5**), 2-methoxystyrene, *o*-$CH_2{=}CHC_6H_4OMe$ (**6**), and 3-butenylmethyl ether, $CH_2{=}CHCH_2CH_2OCH_3$ (**7**) gives the corresponding bis(acetylacetonato)ruthenium(II) complexes [Ru(acac)$_2$(LL′)] (**8**−**14**). These undergo one-electron oxidation by cyclic voltammetry to the corresponding cations [Ru(acac)$_2$(LL′)]$^+$, the process being reversible at both room temperature and −60 °C. The cations were isolated as deep blue, paramagnetic PF_6 or SbF_6 salts from the oxidation of the ruthenium(II) precursors **8**−**12** and **14** with Ag^+ or $[FeCp_2]^+$ salts; they are the first stable alkene complexes of ruthenium(III). At both oxidation levels, coordination of the prochiral alkene gives rise to a pair of diastereomers, labeled **a**, **b** at the Ru(II) level, **a**$^+$, **b**$^+$ at the Ru(III) level, whose redox potentials $E_{1/2}$ (Ru$^{3+/2+}$) differ by ca. 100 mV. The equilibrium **a**/**b** ratio at the Ru(II) level is ca. 1:9, although for **8**, **10**, and **11** this is established only after several hours at ca. 100 °C, the ratio in the complexes immediately after isolation being ca. 2:3. Selective removal of the more easily oxidized diastereomer of the 2-vinyl-*N*,*N*-dimethylaniline complex **8a** by treatment of a 2:3 mixture with ca. 0.5 equiv of Ag^+ provides pure **8b**, which undergoes reversible one-electron oxidation at −60 °C to **8b**$^+$. Above −10 °C, **8b**$^+$ isomerizes to an equilibrium mixture (ca. 85:15) of **8a**$^+$ and **8b**$^+$, as shown by UV−visible spectroelectrochemistry. Thus, both diastereomeric preference and rate of interconversion are strongly dependent on the oxidation state (number of metal d-electrons). The metrical parameters pertaining to alkene coordination in the diastereomers **8a** and **8b** do not differ significantly, the metal−carbon distances being 2.159(4), 2.144(4) Å (**8a**), 2.142(2), 2.153(3) Å (**8b**) and the C═C distances being 1.383(5) Å (**8a**) and 1.382(4) Å (**8b**). The corresponding distances in the Ru(III) complex [**8a**]$^+$[SbF$_6$]$^-$ [Ru−C = 2.239(6), 2.236(7) Å; C═C = 1.355(9) Å] indicate that the alkene is more weakly bound than in either of its diastereomeric Ru(II) precursors.

Introduction

Although the active center of the original titanium-based Ziegler−Natta catalysts for ethylene polymerization is believed to be trivalent titanium,[1−3] alkene complexes of Ti(III) (3d^1) have not been isolated or detected. The few known, well-characterized, paramagnetic alkene or unconjugated diene complexes contain 3d- elements, e.g., [V(CO)$_4$(LL′)](LL′ = *o*-$CH_2{=}CHCH_2C_6H_4PPh_2$, *E*-*o*-$CH_3CH{=}CHC_6H_4PPh_2$),[4] [V(η^5-C_5H_5)$_2$ (*E*-$MeO_2CH{=}CHCO_2Me$)],[5−7] [Fe(PEt$_3$)$_2$(C$_2$H$_4$)$_2$],[8] [Co(PR$_3$)$_3$(C$_2$H$_4$)] (R = Me,[9−11] Ph[12]), [Co(PMe$_3$)$_2$(COD)] (COD = 1,5-cyclooctadiene),[11] [Co(NCMe)$_2$ (*E*-$EtO_2CCH{=}CHCO_2Et$))$_2$],[13] and [{NiX(COD)}$_2$] (X = Br, I).[14,15] No mononuclear alkene complexes having the same composition and stereochemistry but differing only in the oxidation state and electron configuration of the transition metal atom have been isolated; hence, the effect of changes in these parameters on metal-alkene bonding cannot be assessed. A couple based on Ru(II) (4d^6)

---

(1) Gates, B. C.; Katzer, J. R.; Schuit, G. C. A. *Chemistry of Catalytic Processes*; McGraw-Hill: New York, 1979; p 160.

(2) Boor, J., Jr. *Ziegler−Natta Catalysts and Polymerizations*; Academic: New York, 1979; p 266.

(3) Gavens, P. D.; Bottrill, M.; Kelland, J. W.; McMeeking, J. In *Comprehensive Organometallic Chemistry*; Wilkinson, G., Stone, F. G. A., Abel, E. W., Eds.; Pergamon: Oxford, 1982; pp 488−502.

(4) Interrante, L. V.; Nelson, G. V. *J. Organomet. Chem.* **1970**, *25*, 153.

(5) Fachinetti, G.; Del Nero, S.; Floriani, C. *J. Chem. Soc., Dalton Trans.* **1976**, 1046.

(6) Fachinetti, G.; Floriani, C.; Chiesi-Villa, A.; Guastini, C. *Inorg. Chem.* **1979**, *18*, 2282.

(7) Morán, M.; Santos-Garcia, J. J.; Masaguer, J. R.; Fernández, V. *J. Organomet. Chem.* **1985**, *295*, 327.

(8) Hoberg, H.; Jenni, K.; Angermund, K.; Krüger, C. *Angew. Chem., Int. Ed. Engl.* **1987**, *26*, 153.

(9) Klein, H.-F. *Angew Chem., Int. Ed. Engl.* **1980**, *19*, 362.

(10) Klein, H.-F.; Gross, J.; Bassett, J.-M.; Schubert, U. *Z. Naturforsch. B* **1980**, *35*, 614.

(11) Klein, H.-F.; Gross, J.; Witty, H.; Neugebauer, D. *Z. Naturforsch. B* **1984**, *39*, 643.

(12) Kubo, Y.; Pu, L.-S.; Yamamoto, A.; Ikeda, S. *J. Organomet. Chem.* **1975**, *84*, 369.

(13) Agnes, G.; Bassi, I. W.; Benedicenti, C.; Intrito, R.; Calcaterra, M.; Santini, C. *J. Organomet. Chem.* **1977**, *129*, 401.

(14) Porri, L.; Vitulli, G.; Gallazzi, M. C. *Angew. Chem., Int. Ed. Engl.* **1967**, *6*, 452.

(15) Hoberg, H.; Radine, K.; Krüger, C.; Romão, M. J. *Z. Naturforsch. B* **1985**, *40*, 607.

S0002-7863(97)03282-4 CCC: $15.00

and Ru(III) ($4d^5$) would appear to be ideal for this purpose because of the existence of a wide range of configurationally stable, octahedrally coordinated complexes in both oxidation states that are connected by reversible one-electron transfer. Unfortunately, although alkene complexes of octahedral ruthenium(II) are known,[16] their ruthenium(III) counterparts appear to be very unstable. Studies by cyclic voltammetry and differential pulse polarography have shown that the complexes $[Ru(NH_3)_5(alkene)]^{2+}$ in aqueous solution exhibit quasi-reversible or irreversible one-electron oxidation, $E_{1/2}$ ($Ru^{3+/2+}$) being in the range +0.94−0.98 V vs NHE for the ethylene, isobutene, styrene, and η^2-1,3- butadiene complexes. The alkene in the resulting ruthenium (III) cations is replaced rapidly by water.[17−19] The corresponding $[Os(NH_3)_5(alkene)]^{2+}$ complexes are oxidized electrochemically more readily than the analogous ruthenium compounds [$E_{1/2}$ ($Os^{3+/2+}$) 0.35−0.45 V vs NHE],[18−20] and although the presumed osmium(III) cations $[Os(NH_3)_5(alkene)]^{3+}$ readily lose the alkene in the presence of water or dimethylacetamide, a transient pink species believed to be the styrene-osmium(III) complex has been observed.[19] Aquaruthenium(II) alkene complexes of the type $[Ru(H_2O)_n(alkene)_{6-n}]^{2+}$ (n = 4, 5)[21−23] have also been shown by cyclic voltammetry to undergo one-electron oxidation, presumably to the corresponding ruthenium(III) cations. Species of this type have been proposed as intermediates in the ring-opening metathesis polymerization (ROMP) of 7-oxanorbornene derivatives by ruthenium(III) salts.[22]

The complexes *cis*-$[Ru(acac)_2(C_8H_{14})(L)]$ (L = NH_3, $SbPh_3$; C_8H_{14} = cyclooctene; acac = acetylacetonato = 2,4-pentanedionato)[24] show reversible one-electron oxidation by cyclic voltammetry in CH_2Cl_2 at room temperature, and the reduction potentials $E_{1/2}$ ($Ru^{3+/2+}$) are more favorable by ca. 0.5 V for stabilizing Ru(III) relative to Ru(II) than those in the $[Ru(NH_3)_5(alkene)]^{3+/2+}$ couple.[25] Although the ruthenium(III) cations can be detected spectroelectrochemically, attempts to isolate them in a pure state have failed so far, apparently owing to the lability of cyclooctene coordinated to ruthenium(III). An obvious way to circumvent this difficulty is to link the alkene with an N- or O-σ-donor in a chelate group, so that the alkene is tied more firmly in the coordination sphere.[26] Here we describe $Ru^{II}(acac)_2$ complexes of this type containing the ligands (LL′) 2-vinyl-*N*,*N*-dimethylaniline, *o*-$CH_2{=}CHC_6H_4NMe_2$ (**1**), 2-isopropenyl-*N*,*N*-dimethylaniline, *o*-$CH_2{=}C(CH_3)C_6H_4NMe_2$ (**2**), 3-butenyldimethylamine, $CH_2{=}CHCH_2CH_2NMe_2$ (**3**), 2-allylpyridine, $CH_2{=}CHCH_2C_5H_4N$ (**4**), isomesityl oxide (4-methyl-4-penten-2-one), $CH_2{=}C(CH_3)CH_2COCH_3$ (**5**), 2-methoxystyrene, *o*-$CH_2{=}CHC_6H_4OMe$ (**6**), and 3-butenylmethyl ether, $CH_2{=}CHCH_2CH_2OMe$ (**7**) and show that they can be oxidized to the first stable, paramagnetic ruthenium(III)-alkene complexes.

Experimental Section

General Procedures. All the organometallic compounds were prepared under anaerobic conditions with use of a positive pressure of purified nitrogen or argon and conventional Schlenk-line and syringe techniques. All solvents were freshly degassed by distillation under nitrogen before use. Benzene, ether, hexane, and THF were dried by distillation from sodium/benzophenone/tetraglyme. Dichloromethane was dried over CaH_2 and distilled. The NMR solvents C_6D_6, CD_2Cl_2, and $CDCl_3$ were degassed by several freeze−thaw cycles before use. Column chromatography was performed under nitrogen on degassed silica gel 60. The following instruments were used: Varian Gemini 300BB or VXR300 (^1H NMR, ^{13}C NMR at 75.5 MHz), Perkin-Elmer 683 or 1800 (FT) (IR spectra on solids as KBr disks or Nujol mulls between KBr windows or on solutions in 0.1 mm KBr cells), VG Micromass 7070 (EI mass spectra at 70 ev), and VG ZAB2−SEQ (FAB mass spectra on samples prepared in CH_2Cl_2 and added to a matrix of tetraglyme or 3-nitrobenzyl alcohol). Magnetic susceptibilities were measured between 4 and 300K by Dr. K. S. Murray and Dr. B. Moubaraki (Monash University) on a Quantum Design MPMS SQUID magnetometer. Calibration for field and temperature was checked against a standard palladium sample (field) and $CuSO_4{\cdot}H_2O$ and $Hg[Co(NCS)_4]$ (temperature). The X- and Q-band EPR spectra of ruthenium(III) compounds as polycrystalline solids or frozen glasses were recorded by Dr. R. Bramley on a Varian Associates spectrometer (100 kHz modulation frequency) fitted with an Oxford Instruments helium flow cryostat. The klystron frequency was determined with a Hewlett-Packard Electronic Counter.

Electrochemical measurements in CH_2Cl_2 at various temperatures were performed on a Princeton Applied Research 170 system as described elsewhere.[27] Peak-to-peak separations in cyclic voltammetry (CV) and peak widths in alternating current voltammetry (acV) were assessed for electrochemical reversibility by comparison with the $[FeCp_2]/[FeCp_2]^+$ couple at the same peak current. At room temperature $E_{1/2}$ ($Fe^{3+/2+}$) for this couple was +0.55 V vs Ag/AgCl. Scan rates were typically 100−200 mV s^{-1} for CV and 20 mV s^{-1} for acV. The electronic spectra of the isolated complexes were measured on a Perkin-Elmer λ9 spectrophotometer, and the spectra of electrogenerated species were collected by use of an optically transparent thin layer electrochemical (OTTLE) cell placed in the spectrophotometer, as described previously.[27] Microanalyses were performed in-house. Elemental analyses and mass spectra are listed in Table 1; ^1H and ^{13}C NMR data are collected in Table 2.

The following starting materials were prepared by the appropriate literature procedures: liquid zinc amalgam (2−3% Zn),[28] $[FeCp_2]PF_6$,[29] $[Ru(acac)_3]$,[30−32] 2-vinyl-*N*,*N*-dimethylaniline (**1**),[33] 3-butenyldimethylamine (**3**),[34] 2-allylpyridine (**4**),[35] isomesityl oxide (**5**),[36] and 2-methoxystyrene (**6**).[37] 2-Isopropenyl-*N*,*N*-dimethylaniline (**2**) (bp 64 °C/6

---

[16] (a) Bennett, M. A.; Bruce, M. I.; Matheson, T. W. In *Comprehensive Organometallic Chemistry*; Wilkinson, G., Stone, F. G. A., Abel, E. W., Eds.; Pergamon: Oxford, 1982; Vol. 4, p 741. (b) Bennett, M. A. In *Comprehensive Organometallic Chemistry II*; Abel, E. W., Stone, F. G. A., Wilkinson, G., Eds.; Shriver, D. F., Bruce, M. I., Vol. Ed.; Pergamon: Oxford, 1995; Vol. 7, p 441.

[17] Lehmann, H.; Schenk, K. J.; Chapuis, G.; Ludi, A. *J. Am. Chem. Soc.* **1979**, *101*, 6197.

[18] Elliott, M. G.; Shepherd, R. E. *Inorg. Chem.* **1988**, *17*, 3332.

[19] Elliott, M. G.; Zhang, S.; Shepherd, R. E. *Inorg. Chem.* **1989**, *28*, 3036.

[20] Harman, W. D.; Taube, H. *J. Am. Chem. Soc.* **1988**, *110*, 7906.

[21] Laurenczy, G.; Merbach, A. E. *J. Chem. Soc., Chem. Commun.* **1993**, 187.

[22] Novak, B. M.; Grubbs, R. H. *J. Am. Chem. Soc.* **1988**, *110*, 7542.

[23] McGrath, D. V.; Grubbs, R. H.; Ziller, J. W. *J. Am. Chem. Soc.* **1991**, *113*, 3611.

[24] Bennett, M. A.; Chung, G.; Neumann, H., to be published.

[25] Wallace, L. Ph.D. Thesis, Australian National University, Canberra; 1991.

[26] Hall, D. I.; Ling, J. H.; Nyholm, R. S. *Struct. Bonding* **1973**, *15*, 3.

[27] Duff, C. M.; Heath, G. A. *Inorg. Chem.* **1991**, *30*, 2528; *J. Chem. Soc., Dalton Trans.* **1991**, 2401.

[28] Brauer, G. *Handbook of Preparative Inorganic Chemistry*; Academic: New York, 1965; Vol. 2, p 1806.

[29] Brauer, G. *Handbuch der Präparativen Anorganischen Chemie*; Ferdinand Enke: Stuttgart, 1981; Vol. 3, p 1845.

[30] Gordon, J. G. II; O'Connor, M. J.; Holm, R. H. *Inorg. Chim. Acta* **1971**, *5*, 381.

[31] Earley, J. E.; Base, R. N.; Berrie, B. H. *Inorg. Chem.* **1983**, *22*, 1836.

[32] Knowles, T. S.; Howells, M. E.; Howlin, B.; Smith, G. W.; Amodio, C. A. *Polyhedron* **1994**, *13*, 2197.

[33] Booth, H.; King, F. E.; Parrick, J. *J. Chem. Soc.* **1958**, 2302.

[34] Angermund, K.; Bogdanović, B.; Koppetsch, G.; Krüger, C.; Mynott, R.; Schwickardi, M.; Tsay, Y. H. *Z. Naturforsch., B* **1986**, *41*, 455.

[35] (a) Troyanowsky, C. *Bull. Soc. Chim. Fr.* **1955**, 420. (b) Yingst, R. E.; Douglas, B. E. *Inorg. Chem.* **1964**, *3*, 1177. (c) Israeli, M.; Laing, D. K.; Pettit, L. D. *J. Chem. Soc., Dalton Trans.* **1974**, 2194. (d) Heaton, B. T.; McCaffrey, D. J. A. *J. Chem. Soc., Dalton Trans.* **1979**, 1078.

[36] Stross, F. H.; Monger, J. M.; Finch, H. de V. *J. Am. Chem. Soc.* **1947**, *69*, 1627.

[37] Redeuilh, G.; Rumpf, P.; Viel, C. *Bull. Soc. Chim. Fr.* **1973**, 2665.

Table 1. Elemental Analysis and Mass Spectra for $[Ru(acac)_2(LL')]$ and $[Ru(acac)_2(LL')]PF_6$[a]

compd	Anal. [calcd(found)] %C	%H	%N	*m*/*z* (intensity %)[b]
8	53.80 (53.65)	6.09 (6.66)	3.14 (2.95)	447 (56) (*M*), 300 (100), 147 (21)
9	54.77 (54.82)	6.35 (6.53)	3.04 (2.80)	461 (38) (*M*), 300 (47), 161 (9)
10	48.23 (48.15)	6.83 (6.73)	3.52 (3.21)	399 (64) (*M*), 300 (64), 200 (10), 99 (71)
11	51.67 (51.51)	5.54 (5.78)	3.35 (3.26)	419 (61) (*M*), 319 (15), 300 (100), 119 (8)
12	48.35 (48.01)	6.09 (6.20)		398 (21) (*M*), 300 (73), 98 (20)
$[\mathbf{8}]^+[PF_6]^-$	40.61 (41.08)	4.60 (4.51)	2.37 (2.34)	447 (100) (*M*), 300 (40)
$[\mathbf{9}]^+[PF_6]^-$	41.66 (41.84)	4.83 (4.58)	2.31 (2.45)	461 (100) (*M*), 300 (59)
$[\mathbf{10}]^+[PF_6]^-$	35.36 (35.68)	5.01 (5.00)	2.58 (2.25)	399 (100) (*M*), 300 (28)
$[\mathbf{11}]^+[PF_6]^-$	38.37 (38.64)	4.11 (4.10)	2.49 (2.58)	419 (28) (*M*), 307 (40), 277 (100)
$[\mathbf{12}]^+[PF_6]^-$	35.43 (35.60)	4.46 (4.70)		398 (100) (*M*), 300 (100)
$[\mathbf{14}]^+[PF_6]^-$ [c]	33.97 (32.71)	4.56 (4.45)		*d*

[a] EI-MS for neutral compounds, FAB-MS for salts. [b] **13**: *m*/*z* 434 (0.1), 300 (0.2), 134 (20); **14**: *m*/*z* 386 (0.4), 300 (0.9), 86 (29). [c] %P calcd, 5.84; found, 5.70. [d] Not measured.

Torr) was prepared from 2-isopropenylaniline,[38] following the procedure for the synthesis of 2-iodo-*N*,*N*-dimethylaniline from 2-iodoaniline.[39] 3-Butenylmethyl ether (**7**)[34] was prepared by reaction of the sodium salt of commercially available 3-buten-1-ol with dimethyl sulfate.

Preparations. Bis(acetylacetonato)(2-vinyl-*N*,*N*-dimethylaniline)ruthenium(II), 8. A mixture of $[Ru(acac)_3]$ (2.0 g, 5.0 mmol) and 2-vinyl-*N*,*N*-dimethylaniline (**1**) (0.74 g, 5.0 mmol) in THF (160 mL) containing water (3 mL) was heated under reflux for 2 h in the presence of zinc amalgam (ca. 10 mL) to give a yellow-orange suspension. Filtration and removal of solvents under reduced pressure gave an orange oily residue, which contained ca. 55% of **8a** and 45% of **8b** according to ^1H NMR spectroscopy. Column chromatography on silica gel in 3:1 THF/hexane gave one orange fraction; a small amount of red-brown material remained on the column. Evaporation gave **8** as yellow-orange solid, which was washed with a few milliliters of cold ether and dried in vacuo at 60 °C for 2 h. The yield of **8** was 1.9 g (85%); the ratio of **8a** to **8b** was ca. 2:3. X-ray quality crystals of **8a** were obtained as the first crop from a solution of this isomeric composition in hexane after several days at 0 °C. Crystals of **8b** were obtained similarly from an ether solution of isomeric composition **8a**:**8b** of ca. 1:9 obtained by the selective oxidation procedure described below.

The other $Ru^{II}(acac)_2$ complexes **9**−**14** were obtained similarly after chromatography as isomeric mixtures by addition of hexane to concentrated THF solutions. Yields of isolated compounds were 40−80%.

Bis(acetylacetonato)(2-vinyl-*N*,*N*-dimethylaniline)ruthenium(III) Salts, $[\mathbf{8}]^+Y^-$ ($Y = PF_6$, SbF_6). A solution of **8** (205 mg, 0.46 mmol) in CH_2Cl_2 (40 mL) was treated with an excess of $AgPF_6$ (174 mg, 0.69 mmol) to give a suspension in a deep blue solution, which was stirred for 3 h and filtered through Celite. The filtrate was evaporated to dryness, and the fluffy solid residue was redissolved in a few milliliters of CH_2Cl_2. Addition of ether precipitated the deep blue, microcrystalline salt $[\mathbf{8}]^+[PF_6]$, which was washed with ether (10 mL) and dried at 50 °C in vacuo for 3 h. The yield was 0.24 g (89%). It contained ca. 70% of $\mathbf{8a}^+$ and 30% of $\mathbf{8b}^+$, as shown by alternating current voltammetry. Reduction of the solution with NaOMe in methanol gave **8a** and **8b** in ca. 7:3 ratio, according to ^1H NMR spectroscopy. Use of $AgSbF_6$ in place of $AgPF_6$ gave a CH_2Cl_2 solution from which X-ray quality crystals of $[\mathbf{8a}]^+[SbF_6]^-$ were obtained by layering with hexane.

The other $Ru^{III}(acac)_2$ salts $\mathbf{9}^+$−$\mathbf{12}^+$ and $\mathbf{14}^+$ were isolated as described above in 80−90% yield.

Selective Oxidation. A solution containing **8** (**a**:**b** ca. 45:55) (340 mg, 0.76 mmol) in CH_2Cl_2 (30 mL) was treated with solid $AgPF_6$ (106 mg, 0.42 mmol), and the mixture was stirred for 3 h at room temperature. The green-blue solution was filtered through Celite, the filtrate was evaporated to dryness, and the residue was extracted with ether (3 × 10 mL) to give an orange solution and a deep blue solid. Removal of the solvent from the extract gave an oily residue, which contained ca. 90% of **8b**. Crystallization from a few milliliters of ether at 0 °C gave pure **8b** (70 mg, 21% yield).

Pure **11b** was obtained similarly in 36% yield from a sample of the 2-allylpyridine complex **11** (**a**:**b** ca. 40:60).

X-ray Crystallography. Crystal data and details of data collection, data processing, structure analysis, and structure refinement are in Table 3. Lattice parameters were determined by least-squares refinement of the setting angles of 25 reflections in the range $39.83 < 2\theta < 47.77°$ for **8a**, $50.04 < 2\theta < 53.39°$ for **8b**, and $33.66 < 2\theta < 38.65°$ for $[\mathbf{8a}]SbF_6$.

Results

Synthesis and Characterization of Ruthenium Complexes. Reduction of $[Ru(acac)_3]$ by zinc amalgam in refluxing THF containing a small amount of water in the presence of an excess of ligands **1**−**7** (LL′)[45] gave complexes of empirical formula $[Ru(acac)_2(LL')]$ (**8**−**14**) as orange or brown solids in isolated yields of 40−80%. Complexes **8**−**12** are stable to air, whereas **13**−**14**, derived from unsaturated ethers, are highly air-sensitive, especially in solution. All the complexes show a parent-ion peak in their EI-mass spectra. The IR spectra exhibit two intense bands in the regions 1585−1570 cm^{-1} and 1525−1510 cm^{-1} characteristic of bidentate O-bonded acac.[50] There are no bands in the region 1620−1640 cm^{-1} assignable to $\nu(C{=}C)$ of an uncoordinated alkene. By analogy with the $[Ru(NH_3)_5(alkene)]^{2+}$ complexes,[17] the $\nu(C{=}C)$ band due to the coordinated double bond would be expected to appear in the range 1550−1490 cm^{-1} and is likely to be masked by the intense acac absorption.

---

(38) Atkinson, C. M.; Simpson, J. C. E. *J. Chem. Soc.* **1947**, 808.

(39) Baeyer, A. *Ber.* **1905**, *38*, 2759.

(40) *teXsan: Single-Crystal Structure Analysis Software*, Versions 1.6c and 1.7; Molecular Structure Corp.: The Woodlands, TX, 1993 and 1995.

(41) Cromer, D. T.; Waber, J. T. *International Tables for X-ray Crystallography*; Kynoch Press: Birmingham, England, 1974; Vol IV.

(42) *International Tables for Crystallography*; Kluwer Academic: Boston, MA, 1992; Vol. C, Tables 4.2.4.3 and 4.2.6.8.

(43) Fan, Hai-Fu. SAPI 91. *Structure Analysis Programs with Intelligent Control*; Rigaku Corporation, Tokyo, Japan, 1991.

(44) Beurskens, P. T.; Admiraal, G.; Beurskens, G.; Bosman, W. P.; Garcia-Granda, S.; Gould, R. O.; Smits, J. M. M.; Smykalla, C. The DIRDIF-92 Program System. Technical Report of the Crystallography Laboratory; University of Nijmegen, The Netherlands, 1992.

(45) Similar procedures have been used to generate $[Ru(acac)_2(NCMe)_2]$,[46] $[Ru(acac)_2(\eta^2\text{-alkene})_2]$,[24] $[Ru(acac)_2(\eta^4\text{-1,3-diene})]$,[47,48] and $[Ru(acac)_2((1,2,5,6\text{-}\eta\text{-}C_8H_8)]$[49] from $[Ru(acac)_3]$.

(46) Kobayashi, T.; Nishina, Y.; Shimizu, K.; Sato, G. P. *Chem. Lett.* **1988**, 1137.

(47) Ernst, R. D.; Meléndez, E.; Stahl, L.; Ziegler, M. L. *Organometallics* **1991**, *10*, 3635.

(48) Meléndez, E.; Ilarraza, R.; Yap, G. P. A.; Rheingold, A. L. *J. Organomet. Chem.* **1996**, *522*, 1.

(49) Bennett, M. A.; Neumann, H.; Willis, A. C.; Ballantini, V.; Pertici, P.; Mann, B. E. *Organometallics* **1997**, *16*, 2868.

(50) Nakamoto, K. *Infrared and Raman Spectra of Inorganic and Coordination Compounds*, 3rd ed.; Wiley: New York, 1978; p 249.

Table 2. ^{1}H and ^{13}C NMR Data for Ligands (LL′) and [Ru(acac)$_2$(LL′)] Complexes[a,b]

compd	^{1}H NMR (δ)[c]	^{13}C NMR (δ)[d]
1	7.21 (dd, H^3), 5.59 (dd, H^2), 5.11 (dd, H^1) ($J_{23} = 17.8$, $J_{13} = 11.0$, $J_{12} = 1.7$); 2.41 (s, NMe_2)	135.5 (C^2), 112.9 (C^1); 44.5 (NMe_2)
8a	5.39 (dd, H^3), 5.06 (d, H^1), 4.64 (d, H^2) ($J_{23} = 11.3$, $J_{13} = 8.8$, $J_{12} \sim 0$); 5.55 (s), 4.94 (s) (CH of acac), 2.13 (s), 1.90 (s), 1.72 (s), 1.67 (s) (CH_3 of acac); 2.90 (s), 1.94 (s) (NMe_2)	84.7 (C^2), 77.9 (C^1); 187.7, 187.5, 185.5, 184.9 ($C{=}O$), 99.9, 98.1 (CH of acac), 28.4, 27.7, 27.2 (CH_3 of acac); 54.1, 52.8 (NMe_2)
8b	6.40 (dd, H^3), 4.30 (d, H^1), 3.58 (d, H^2) ($J_{23} = 11.3$, $J_{13} = 9.6$, $J_{12} \sim 0$); 5.48 (s), 5.46 (s) (CH of acac), 2.15 (s), 1.87 (s), 1.84 (s), 1.83 (s) (CH_3 of acac); 2.58 (s), 2.54 (s) (NMe_2)	89.4 (C^2), 72.2 (C^1); 188.8, 185.5, 185.3, 185.2 ($C{=}O$), 99.9, 99.4 (CH of acac), 28.5, 28.0, 27.5 (CH_3 of acac); 55.5, 50.4 (NMe_2)
2	5.16 (m, H^2), 5.08 (m, H^1); 2.53 (s, NMe_2), 2.21 (s, $\mathrm{C}\mathit{Me}{=}\mathrm{CH_2}$)	137.3 (C^2), 114.2 (C^1); 43.3 (NMe_2), 21.6 ($\mathrm{C}\mathit{Me}{=}\mathrm{CH_2}$)
9a	5.12 (s, H^2), 4.62 (s, H^1); 5.52 (s), 5.04 (s) (CH of acac), 2.83, 2.14, 1.93, 1.91, 1.80, 1.79, 1.69 (each s, 3H, acac CH_3, NMe_2, $\mathrm{C}\mathit{Me}{=}\mathrm{CH_2}$)	89.7 (C^2), 77.8 (C^1); 187.4, 185.4, 184.7 ($C{=}O$), 99.5, 98.7 (CH of acac), 28.5, 27.9, 27.1 (CH_3 of acac); 54.4, 53.2 (NMe_2); 22.5 ($\mathrm{C}\mathit{Me}{=}\mathrm{CH_2}$)
9b	4.16 (s, H^1), 3.44 (s, H^2); 5.50 (s), 5.37 (s) (CH of acac); 2.13 (s), 1.96 (s), 1.80 (s), 1.77 (s) (CH_3 of acac); 2.43 (s), 2.41 (s) (NMe_2); 2.36 (s, $\mathrm{C}\mathit{Me}{=}\mathrm{CH_2}$)	89.5 (C^2), 72.7 (C^1); 188.6, 186.0, 185.4, 184.8 ($C{=}O$), 99.9, 99.2 (CH of acac), 28.6, 28.1, 27.8, 27.5 (CH_3 of acac); 54.6, 52.4 (NMe_2); 24.2 ($\mathrm{C}\mathit{Me}{=}\mathrm{CH_2}$)
3	5.81 (m, H^3), 5.09-4.97 (m, H^1, H^2); 2.25−2.10 (m, $2CH_2$), 2.06 (s, NMe_2)	137.3 (C^2), 115.3 (C^1); 59.4 (CH_2N), 32.7 ($\mathit{C}\mathrm{H_2CH}$), 45.4 (NMe_2)
10a	4.51 (m, H^1, H^2, H^3); 5.52 (s), 4.90 (s) (CH of acac); 2.48−1.70 (m, $2CH_2$); 2.40, 2.09, 1.92, 1.81, 1.67, 1.42 (each s, 3H, CH_3 of acac, NMe_2)	86.6 (C^2), 74.5 (C^1); 187.2, 185.0, 184.8, 184.5 ($C{=}O$), 99.8, 98.0 (CH of acac), 28.4, 28.1, 27.9, 27.3 (CH_3 of acac); 66.6 (CH_2N), 31.2 ($\mathit{C}\mathrm{H_2CH}$); 50.7, 50.4 (NMe_2)
10b	5.35 (m, H^3), 4.09 (d, H^1), 3.29 (d, H^2) ($J_{23} = 12.1$, $J_{13} = 8.5$, $J_{12} \sim 0$); 5.52 (s), 5.43 (s) (CH of acac); 2.48−1.70 (m, $2CH_2$); 2.08 (s, 3H), 2.04 (s, 3H), 1.96 (s, 6H), 1.90 (s, 3H), 1.84 (s, 3H) (CH_3 of acac, NMe_2)	90.3 (C^2), 71.2 (C^1); 187.7, 186.8, 185.2, 184.5 ($C{=}O$), 99.9, 99.2 (CH of acac), 28.5, 28.2, 28.0, 27.7 (CH_3 of acac); 67.2 (CH_2N), 30.2 ($\mathit{C}\mathrm{H_2CH}$); 50.0, 49.8 (NMe_2)
4[e]	8.60−7.25 (m, C_5H_4); 6.06 (m, H^3), 5.17 (m, H^2), 5.14 (m, H^1) ($J_{23} = 17.1$, $J_{13} = 11.0$, $J_{12} = 3.0$); 3.60 (m, CH_2)	160.0−121.3 (C_5); 135.7 (C^2), 116.9 (C^1); 42.8 (CH_2)
11a	8.91−6.21 (m, C_5H_4); 5.22 (m, H^3), 4.80 (d, H^2), 4.46 (d, H^1) ($J_{23} = 12.1$, $J_{13} = 8.1$, $J_{12} \sim 0$); 3.72 (dd), 3.18 (dd) (CH_2); 5.36 (s), 5.07 (s) (CH of acac), 2.21 (s), 1.92 (s), 1.77 (s), 1.69 (s) (CH_3 of acac)	174.0, 152.1, 134.1, 120.0 (C_5H_4); 87.9 (C^2), 75.2 (C^1); 43.5 (CH_2); 187.0, 185.7, 184.1 ($C{=}O$), 99.3, 98.2 (CH of acac), 28.6, 28.1 (CH_3 of acac)
11b	8.69−6.21 (m, C_5H_4); 5.68 (m, H^3), 4.29 (d, H^1), 3.48 (d, H^2) ($J_{23} = 12.0$, $J_{13} = 8.1$, $J_{12} \sim 0$); 3.94 (dd), 3.15 (dd) (CH_2); 5.47 (s), 5.42 (s) (CH of acac), 2.20 (s), 1.96 (s), 1.92 (s), 1.83(s) (CH_3 of acac)	173.1, 151.9, 133.9, 120.9, 120.1 (C_5H_4); 86.9 (C^2), 71.9 (C^1); 42.8 (CH_2); 188.8, 186.1, 185.7, 184.9 ($C{=}O$), 99.6, 99.4 (CH of acac), 28.8, 28.7, 28.5, 28.3 (CH_3 of acac)
5[e]	4.97 (m, H^2), 4.83 (m, H^1), 3.13 (s, CH_2), 2.17 (s, $\mathrm{C}\mathit{Me}{=}\mathrm{CH_2}$), 1.76 (s, CO*Me*)	139.4 (C^2), 115.3 (C^1); 207.1 (*C*OMe), 53.3 (CH_2), 29.3 (CO*Me*), 22.7 ($\mathrm{C}\mathit{Me}{=}\mathrm{CH_2}$)
12b[f]	3.73 (d, H^1), 3.33 (d, H^2), 3.86 (d), 2.72 (d) (CH_2), 5.53(s), 5.45(s) (CH of acac), 2.35, 2.26, 2.00, 1.98, 1.92, 1.79 (each s, 3H, CH_3 of acac, COMe, $\mathrm{C}\mathit{Me}{=}\mathrm{CH_2}$)	93.5 (C^2), 75.1 (C^1); 229.7 (*C*OMe), 59.5 (CH_2); 189.0, 185.9, 185.7, 185.6 ($C{=}O$), 99.5, 98.6 (CH of acac), 29.2, 28.2, 27.5, 27.4, 27.3 (CH_3 of acac, *Me*CO); 24.5 ($\mathrm{C}\mathit{Me}{=}\mathrm{CH_2}$)
6	7.33 (dd, H^3), 5.75 (d, H^2), 5.22 (d, H^1) ($J_{23} = 17.6$, $J_{13} = 11.3$, $J_{12} = 1.6$), 3.27 (s, OMe)	132.2 (C^2), 114.2 (C^1), 54.9 (OMe)
13a	5.88 (m, H^3), 5.40 (d, H^2), 5.25 (d, H^1) ($J_{23} = 12.0$, $J_{13} = 8.7$, $J_{23} \sim 0$), 3.10 (s, OMe); 5.59 (s), 5.33 (s) (CH of acac), 1.98 (s), 1.93 (s), 1.78 (s), 1.60 (s) (CH_3 of acac)	86.1 (C^2), 77.9 (C^1), 60.4 (OMe); 99.4, 98.6 (CH of acac)
13b	6.78 (m, H^3), 4.60 (d, H^1), 4.00 (d, H^2) ($J_{23} = 11.8$, $J_{13} = 8.8$, $J_{12} \sim 0$), 3.39 (s, OMe); 5.57 (s), 5.48 (s) (CH of acac), 2.25 (s), 1.96 (s), 1.88 (s), 1.77 (s) (CH_3 of acac)	91.1 (C^2), 73.6 (C^1), 59.3 (OMe); 190.0, 186.7, 185.7, 185.6 ($C{=}O$), 100.5, 99.8 (CH of acac), 28.4, 27.9, 27.5, 26.9 (CH_3 of acac)
7	5.75 (m, H^3), 5.27 (m, H^2), 4.97 (m, H^1), 3.08 (s, OMe), 3.19 (t), 2.20 (m) ($2CH_2$)	135.7 (C^2), 116.1 (C^1), 72.2 (CH_2O), 34.6 ($\mathit{C}\mathrm{H_2CH}$), 58.2 (OMe)
14a	5.39 (d, H^2), 5.22 (m, H^3), 4.60 (d, H^1) ($J_{23} = 12.4$, $J_{13} = 8.1$, $J_{12} \sim 0$); 5.55 (s), 4.87 (s) (CH of acac); 3.01 (s, OMe); 3.40−1.40 (m, $2CH_2$); 2.25 (s), 1.90(s), 1.78 (s), 1.67 (s) (CH_3 of acac)	92.1 (C^1), 83.3 (C^1); 188.8, 185.8, 185.3, 185.0 ($C{=}O$), 101.0, 98.2 (CH of acac), 28.4, 28.0, 27.7, 26.6 (CH_3 of acac); 76.6 (CH_2O), 35.0 ($\mathit{C}\mathrm{H_2CH}$), 62.0 (OMe)
14b	5.92 (m, H^3), 4.26 (d, H^1), 3.90 (d, H^1) ($J_{23} = 11.8$, $J_{13} = 8.2$, $J_{12} \sim 0$); 5.51 (s), 5.49 (s) (CH of acac); 2.94 (s, OMe); 3.35−1.40 (m, $2CH_2$); 2.17 (s), 1.96 (s), 1.93 (s), 1.79 (s) (CH_3 of acac)	93.9 (C^2), 82.8 (C^1); 188.9, 185.6, 185.4, 185.2 ($C{=}O$), 100.4, 99.4 (CH of acac), 28.3, 28.1, 27.6, 27.1 (CH_3 of acac); 74.1 (CH_2O), 35.4 ($\mathit{C}\mathrm{H_2CH}$), 61.7 (OMe)

[a] Measured in C_6D_6, except where stated otherwise; coupling constants (*J*) are in Hz. [b] Atom numbering in vinyl group:

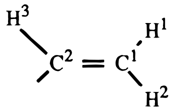

[c] Aromatic resonances were in the region δ 6.4−7.5 for all compounds. [d] Aromatic resonances were in the region δ 120−160 for all compounds. [e] In $CDCl_3$. [f] Proportion of **12a** insufficient to determine ^{1}H and ^{13}C NMR parameters.

The ^{1}H NMR spectra of complexes **8−14** (Table 2) exhibit two groups of resonances in the region δ 1.4−2.3, each consisting of four singlets, due to the acac methyl protons, and two pairs of singlets in the region δ 4.8−5.6 due to the acac methine protons. In some cases, only six or seven methyl singlets are observed owing to overlap. Correspondingly, in

Table 3. Crystal and Refinement Data for the Diastereomers of [Ru(acac)$_2$(*o*-CH$_2$═CHC$_6$H$_4$NMe$_2$)] (**8a** and **8b**) and for [Ru(acac)$_2$(*o*-CH$_2$═CHC$_6$H$_4$NMe$_2$)]SbF$_6$, [**8a**]$^+$[SbF$_6$]$^-$

	8a	**8b**	[**8a**]$^+$[SbF$_6$]$^-$
(a) Crystal Data			
chemical formula	$C_{20}H_{27}NO_4Ru$	$C_{20}H_{27}NO_4Ru$	$C_{20}H_{27}F_6NO_4RuSb$
fw	446.51	446.51	682.25
cryst syst	monoclinic	monoclinic	triclinic
space group	$P2_1/n$ (no. 14)	$P2_1/c$ (no. 14)	$P\bar{1}$ (no. 2)
crystal color, habit	orange, block	orange, block	dark purple, thin plate
a, Å	9.705(1)	11.868(1)	9.125(3)
b, Å	17.781(4)	11.712(3)	11.929(4)
c, Å	11.731(3)	14.622(2)	12.567(3)
α, deg			81.73(2)
β, deg	101.14(2)	101.18(2)	82.03(2)
γ, deg			70.75(2)
V, Å^3	1986.2(6)	1993.9(5)	1271.9(7)
d_{calc}, g cm^{-3}	1.493	1.487	1.781
F (000)	920	920	670
μ[Mo Kα], cm^{-1}	8.13	8.10	17.18
(b) Data Collection and Processing			
diffractometer	Philips PW1100/20	Philips PW1100/20	Rigaku AFC6S
X-radiation	Mo Kα	Mo Kα	Mo Kα
λ, Å	0.710 69	0.710 69	0.710 69
scan mode	$\theta-2\theta$	$\theta-2\theta$	$\theta-2\theta$
ω-scan width	$1.00 + 0.34 \tan\theta$	$1.00 + 0.34 \tan\theta$	$1.50 + 0.34 \tan\theta$
scan rate, deg min^{-1}	2	2	2
$2\theta_{max}$, (deg)	54.9	55.0	55.1
no. of unique data	4584	4587	5880
no. of data refined	3428 [$I > 3\sigma(I)$]	3722 [$I > 3\sigma(I)$]	3192 [$I > 3\sigma(I)$]
no. of variables	236	236	298
abs corr	analytical	analytical	analytical
min, max corr	0.85−0.93	0.77−0.91	0.68−0.96
(c) Structure Analysis and Refinement[a]			
structure soln	direct methods[b]	Patterson (DIRDIF92, PATTY)[c]	Patterson (DIRDIF92, PATTY)[c]
refinement	full-matrix least-squares minimizing $\Sigma w(\lvert F_o\rvert - \lvert F_c\rvert)^2$	full-matrix least-squares minimizing $\Sigma w(\lvert F_o\rvert - \lvert F_c\rvert)^2$	full-matrix least-squares minimizing $\Sigma w(\lvert F_o\rvert - \lvert F_c\rvert)^2$ [d]
p factor[e]	0.013	0.001	
R	0.033	0.027	0.036
R_w	0.036	0.029	0.036
GOF	2.13	1.99	1.16

[a] Calculations were performed by teXsan,[40] with neutral atom scattering factors from ref 41; $\Delta f'$ and $\Delta f''$ values and mass attenuation coefficients were taken from ref 42. [b] Reference 43. [c] Reference 44. [d] $w = 1$. [e] $w = [\sigma^2(F_o) + 0.25\,p^2F_o^2]^{-1}$.

the ^{13}C NMR spectra, there are two sets of four resonances in the region δ 26.6−28.8 due to acac CH$_3$ (sometimes fewer than eight resonances are observed owing to overlap), two pairs of resonances at δ 97.5−101.0 due to acac CH, and two sets of four resonances in the region δ 184−190 assignable to the acac carbonyl groups. Since the Ru(acac)$_2$ complex of an unsymmetrical bidentate ligand would be expected to show four CH$_3$, two CH, and four CO resonances due to acac, it is clear that each complex consists of a pair of isomers.

The ^{1}H NMR spectra of complexes **8**, **10**, **11**, **13**, and **14** show typical ABX patterns due to the vinylic protons H,^{1} H,^{2} H^3 of a pair of isomers (see footnote to Table 2 for numbering). These resonances are generally shielded relative to the corresponding resonances in the spectra of the free ligands **1**, **3**, **4**, **6**, and **7**. Also, the *trans*- and *cis*-vicinal coupling constants J_{23} and J_{13}, which are 16.2−17.8 Hz and 10.2−11.3 Hz, respectively, in the ligands are reduced in each isomer to 10.9−12.6 and 7.3−9.6 Hz, respectively; the geminal coupling constants J_{12} are close to zero in both ligands and complexes. In the ^{13}C NMR spectra of each isomer, the two alkene carbon resonances are shielded by ca. 50 ppm relative to those in the ligands. Hence, in each isomer the vinyl group is coordinated.

As a consequence of coordination, the NMe$_2$ groups of each isomer of **8**−**10** appear as a pair of singlets in both ^{1}H and ^{13}C NMR spectra, the ^{13}C chemical shifts being deshielded by 2−9 ppm relative to those in the free ligands. A similar deshielding occurs in the methoxy ^{13}C resonances of **13** and **14**. The ^{13}C resonance of the carbonyl group of isomesityl oxide in the major isomer of its Ru(acac)$_2$ complex **12** appears at δ 229.7 (cf. δ 207.1 in **5**), and in the IR spectrum of **12** the ν(C═O) band is observed at 1630 cm^{-1} {cf. 1720 cm^{-1} in **5**, 1600 cm^{-1} in [PtCl$_2$·**5**]}.[51,52] Thus in **12** the C═O group is probably coordinated via the oxygen atom.

The spectroscopic evidence indicates that in complexes **8**−**14** the unsaturated ligands are bound as bidentate chelate groups to a *cis*-Ru(acac)$_2$ fragment (Figure 1). As illustrated in Figure 2, diastereomers can arise because of the chirality of both the *cis*-Ru(acac)$_2$ group (Δ and Λ enantiomeric forms) and the coordinated monosubstituted alkene (*R* and *S*).[53] These conclusions have been confirmed by X-ray studies of both isomers, **8a** and **8b**, of the 2-vinyl-*N*,*N*-dimethylaniline complex (see below). It should be noted that each diastereomer exists as a pair of enantiomers (*R*Δ, *S*Λ; *R*Λ, *S*Δ).

The ^{1}H and ^{13}C NMR spectra of the isomers of **8**−**14** show characteristic differences, which can be illustrated for **8**. The chemical shifts (^{1}H, ^{13}C) in C$_6$D$_6$ of the γ-CH(acac) group of

---

(51) Parshall, G. W.; Wilkinson, G. *Inorg. Chem.* **1962**, *1*, 896.

(52) Gillard, R. D.; Heaton, B. T.; Pilbrow, M. F. *J. Chem. Soc. A* **1970**, 353.

(53) Paiaro, G.; Panunzi, A. *J. Am. Chem. Soc.* **1964**, *86*, 5148.

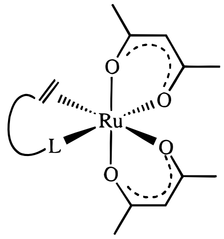

	chelate olefinic ligand (LL')
8	*o*-CH_2=$CHC_6H_4NMe_2$ (**1**)
9	*o*-CH_2=$C(CH_3)C_6H_4NMe_2$ (**2**)
10	CH_2=$CHCH_2CH_2NMe_2$ (**3**)
11	2-CH_2=$CHCH_2C_5H_4N$ (**4**)
12	CH_2=$C(CH_3)CH_2COCH_3$ (**5**)
13	*o*-CH_2=CHC_6H_4OMe (**6**)
14	CH_2=$CHCH_2CH_2OMe$ (**7**)

Figure 1. Chelate alkene complexes [Ru(acac)$_2$(LL′)] (**8**−**14**).

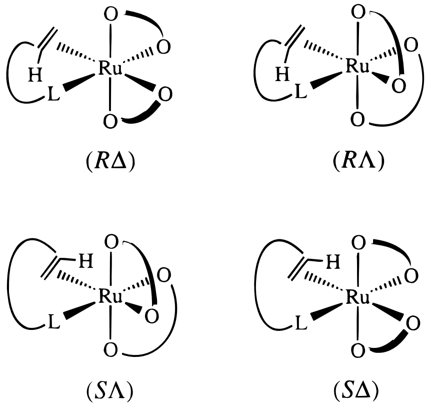

(*R*Δ) (*R*Λ)

(*S*Λ) (*S*Δ)

Figure 2. Isomers of chelate alkene complexes [Ru(acac)$_2$(LL′)].

the less abundant isomer (**8a**) [δ 4.94, 5.55 (^{1}H); 98.1, 99.9 (^{13}C)] are more widely separated than those of the more abundant isomer (**8b**) [δ 5.46, 5.48 (^{1}H); 99.4, 99.9 (^{13}C)]. For both **8a** and **8b**, the order of vinyl group chemical shifts is $\delta(H^3) > \delta(H^1) > \delta(H^2)$, whereas for the free ligand **1** the order is $\delta(H^3) > \delta(H^2) > \delta(H^1)$. However, the shifts resulting from coordination differ markedly, being largest for H^3 in **8a** (1.82 ppm) and largest for H^2 in **8b** (2.01 ppm). Similar regularities are evident for the **a** and **b** isomers of **9**−**14**.

For complexes **8**−**11** containing N-donor vinyl chelate ligands, the **a** and **b** isomers are present in about equal amounts in the isolated products, whereas for the O-donor complexes **12**−**14** the **b** isomers predominate (80−95%). The relative amounts do not change with time at room temperature and are almost unaffected by column chromatography on silica gel. However, when a solid sample containing ca. 55% of **8a** and 45% of **8b** was heated in vacuo at 90 °C, the composition changed continuously with time, being 35%:65% after 24 h and 10%:90% after 72 h. A similar change occurred when a solution of **8** was heated in toluene for 48 h. In the case of **9**, the isomerization seemed to occur more rapidly. Evidently the **b** isomers are thermodynamically more stable than the **a** isomers, and in the case of **8**−**11**, the latter are the kinetic products of the preparation from [Ru(acac)$_3$].

Although the isomers of **8**−**14** could not be separated by column chromatography, two routes to pure **8a** and **8b** were found. First, crystallization of a sample containing ca. 40% **8a** and 60% **8b** from THF/ether gave pure **8a** in the first fraction. Second, as discussed below, **8a** undergoes one-electron oxidation significantly more readily than **8b**. Thus, treatment of **8** (**a**:**b** ca. 45:55) with just 0.5 equiv of AgPF$_6$ gave a mixture consisting mainly of unchanged **8b** and the ruthenium(III) complex [**8a**]$^+$[PF$_6$]$^-$. Extraction with ether gave a mixture containing 90% of **8b** and 10% of **8a**; subsequent recrystallization gave pure **8b**. Attempts to remove the remaining **8a** from the extract by addition of more AgPF$_6$ did not lead to further enrichment. The second procedure was also used to obtain pure **11b** derived from 2-allylpyridine.

Treatment of complexes **8**−**12** and **14** in CH$_2$Cl$_2$ with an equimolar amount of [Fe(C$_5$H$_5$)$_2$]PF$_6$ or, more conveniently, with an excess of silver salts AgX (X = PF$_6$, SbF$_6$) gave ruthenium(III) complexes of general formula [Ru(acac)$_2$(LL′)]X as deep blue solids in up to 90% yield. A similar reaction also occurred in the case of **13**, but the product was not isolated. The ruthenium(III) complexes are stable to air and light, both as solids and in CH$_2$Cl$_2$ solution. The FAB mass spectra show a parent ion peak corresponding to the monomeric ion. In the IR spectra of these compounds [and of Ru(acac)$_3$] there is one broad, intense absorption (70−80 cm^{-1} at half-height) due to acac at ca. 1515 cm^{-1}; there are no bands in the region 1640−1620 cm^{-1} assignable to uncoordinated alkene. In the isomesityl oxide complex [**5**]$^+$[PF$_6$]$^-$ the ν(C=O) band appears at 1632 cm^{-1}, which is similar to the value found in its ruthenium(II) precursor. The magnetic moments at room temperature of [**8**]$^+$[PF$_6$]$^-$ (1.84 μ_B) and [**11**]$^+$[PF$_6$]$^-$ (1.87 μ_B) are similar to that of [Ru(acac)$_3$] (reported values 1.91 μ_B,[54] 1.95 μ_B[55]) and correspond to one unpaired electron. The ESR spectrum of [**11**]$^+$[PF$_6$]$^-$ in a frozen glass (CH$_2$Cl$_2$/CHCl$_3$/THF) at 10 K shows *g*-values of 2.42, 2.03, and 1.85, which are similar to the three components of the *g*-tensor of rhombic symmetry (2.45, 2.16, and 1.45) obtained from studies of [Ru(acac)$_3$] as a single crystal and in frozen solutions.[56] The ESR spectrum of solid [**11**]$^+$[PF$_6$]$^-$ is pseudoisotropic at 285 K ($g = 2.11$) and pseudoaxial at 9 K ($g_1 = 2.18$, $g_2 = 2.04$). The difference between these values and those observed in the frozen glass presumably reflects spin−spin dipole interactions between neighboring paramagnetic centers in the solid state. The evidence indicates that the cations generated by oxidation of **8**−**14** are typical of ruthenium(III) and are not ruthenium(II) species containing a ligand cation radical, for which a *g*-value close to the free-electron value would be expected.

The stability arising from the chelate effect, at least in the N-donor complexes **8**−**11**, is evident from the resistance to displacement of the coordinated alkene, even at the Ru(III) level. The ruthenium(III) complexes are inert toward chloride ion and the ruthenium(II) complexes are unaffected by CO, PMe$_3$, or pyridine. The most common reactions are familiar redox processes, i.e., bases such as methoxide ion effect reduction from Ru(III) to Ru(II), whereas acids cause partial oxidation from Ru(II) to Ru(III).

Crystal Structures. The molecular structures of **8a**, **8b**, and [**8a**]$^+$[SbF$_6$]$^-$ are shown in Figures 3 and 4 and selected metrical parameters are given in Table 4. In **8a** and **8b** the alkene is coordinated symmetrically through its opposite, enantiotopic faces, **8a** containing the *R*Δ/*S*Λ pair and **8b** the *S*Δ/*R*Λ pair; the angle between the planes defined by the atoms Ru, C(19), C(20) and O(3), O(4), C(6), C(8), C(9) is 164° and 45°, respectively. These angles are imposed by the geometry of the chelate ligand. The C=C bond lengths [C(19)−C(20)] are equal

---

[54] Figgis, B. N.; Lewis, J.; Mabbs, F. E.; Webb, G. A. *J. Chem. Soc. A* **1966**, 422.

[55] Buschbeck, C.; Hartmann, H. *Z. Phys. Chem. (Frankfurt)* **1957**, *11*, 120.

[56] De Simone, R. E. *J. Am. Chem. Soc.* **1973**, *95*, 6238.

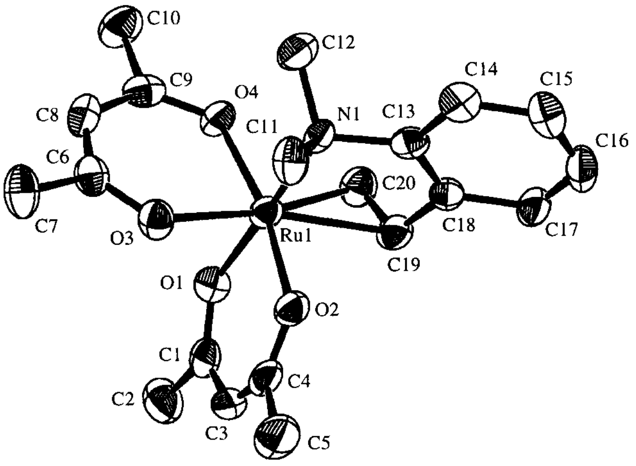

8a

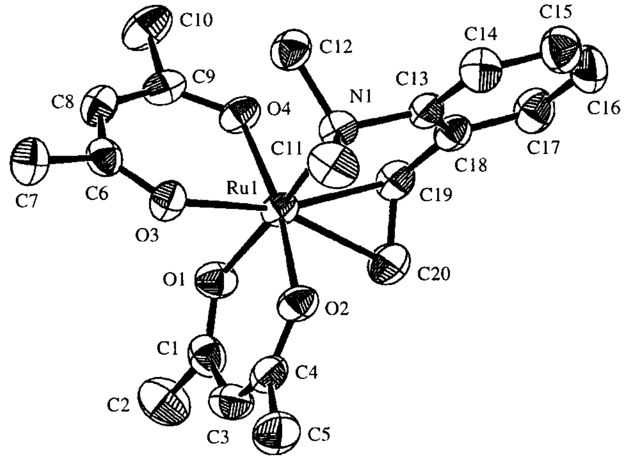

8b

Figure 3. Molecular structures of the diastereomers (*R*Δ and *S*Δ, respectively) of [Ru(acac)$_2$(*o*-CH$_2$=CHC$_6$H$_4$NMe$_2$)] (**8a** and **8b**). Ellipsoids represent 50% probability levels.

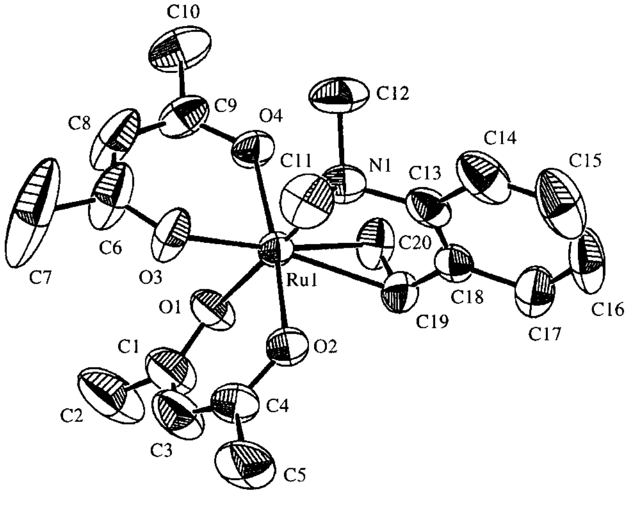

8a⁺

Figure 4. Molecular structure of one diastereomer (*R*Δ) of [Ru(acac)$_2$(*o*-CH$_2$=CHC$_6$H$_4$NMe$_2$)]$^+$ as its SbF$_6$ salt, [**8a**]$^+$ [SbF$_6$]$^-$. Ellipsoids represent 50% probability levels.

Table 4. Selected Interatomic Distances (Å) and Bond Angles (deg) in [Ru(acac)$_2$(*o*-CH$_2$=CHC$_6$H$_4$NMe$_2$)] (**8a** and **8b**) and [Ru(acac)$_2$(*o*-CH$_2$=CHC$_6$H$_4$NMe$_2$)]SbF$_6$, [**8a**$^+$][SbF$_6$]$^-$

compd	**8a**	**8b**	[**8a**]$^+$[SbF$_6$]$^-$
Ru(1)−O(1)	2.055(3)	2.055(2)	1.987(4)
Ru(1)−O(2)	2.064(2)	2.048(2)	2.019(4)
Ru(1)−O(3)	2.077(2)	2.077(2)	2.010(4)
Ru(1)−O(4)	2.074(2)	2.074(2)	2.013(4)
Ru(1)−N(1)	2.159(3)	2.179(2)	2.150(5)
Ru(1)−C(19)	2.159(4)	2.142(2)	2.239(6)
Ru(1)−C(20)	2.144(4)	2.153(3)	2.236(7)
C(19)−C(20)	1.383(5)	1.382(4)	1.355(9)
O(1)−Ru(1)-O(2)	92.2(1)	94.00(7)	90.8(2)
O(1)−Ru(1)-O(3)	87.8(1)	87.46(7)	86.5(2)
O(1)−Ru(1)-O(4)	85.9(1)	82.75(7)	88.6(2)
O(1)−Ru(1)-N(1)	178.9(1)	175.31(7)	178.6(2)
O(2)−Ru(1)-O(3)	80.2(1)	80.56(7)	84.5(2)
O(2)−Ru(1)-O(4)	168.61(9)	169.83(7)	173.8(2)
O(2)−Ru(1)-N(1)	88.3(1)	87.65(7)	88.1(2)
O(3)−Ru(1)-O(4)	88.47(9)	89.65(6)	89.3(2)
O(3)−Ru(1)-N(1)	91.3(1)	88.47(7)	92.5(2)
O(4)−Ru(1)-N(1)	93.4(1)	94.89(7)	92.4(2)
C(19)−Ru(1)-C(20)	37.5(1)	37.53(10)	35.2(2)
C(18)−C(19)-C(20)	120.5(3)	121.1(2)	121.6(6)

within experimental error [1.383(5) Å (**8a**); 1.382(4) Å (**8b**)], cf. 1.381(6) Å in $[\overline{\mathrm{Ru(CH_3CH{=}CHCH_2COO}})_2(\mathrm{OH_2})_2]$[23] and 1.413(8) Å in [Ru(NH$_3$)$_5$ (*E*-HO$_2$CCH=CHCO$_2$H)]$^{2+}$.[17] The metal−carbon distances for **8a** and **8b** also do not differ significantly: **8a**: Ru−C(19) = 2.159(4) Å, Ru−C(20) = 2.144(4) Å; **8b**: Ru−C(19) = 2.142(2) Å, Ru−C(20) = 2.153(3) Å.

The X-ray study of [**8a**]$^+$[SbF$_6$]$^-$ shows unequivocally that the alkene is coordinated, its orientation being the same as that of the minor ruthenium(II) diastereomer **8a**. Since [**8a**]$^+$ is the more abundant and thermodynamically more stable diastereomer at the ruthenium(III) level (see below), the favored alkene orientations clearly differ for Ru(II) and Ru(III). The metal−alkene distances in [**8a**]$^+$[SbF$_6$]$^-$ [Ru−C(19) = 2.239(6) Å, Ru−C(20) = 2.236(7) Å] are 0.06−0.08 Å greater than those in **8a** and **8b**, showing that the alkene is bound more weakly to Ru(III) than to Ru(II). The fact that the C=C bond length in [**8a**]$^+$[SbF$_6$]$^-$ [C(19)−C(20) = 1.355(9) Å] is less than those in **8a** and **8b** is consistent with this suggestion, though the difference is significant only at the 95% confidence level.

The Ru−O distances in [**8a**]$^+$[SbF$_6$]$^-$ are in the range 1.987(4)−2.019(4) Å and are similar to those in the orthorhombic and monoclinic modifications of [Ru(acac)$_3$].[57,58] They are significantly less than the corresponding distances in **8a** [2.055(3)−2.077(2) Å] and **8b** [2.048(2)−2.077(2) Å], consistent with the expected stronger binding of the anionic acac ligand to the higher oxidation state metal ion. The Ru−N distances in **8a** [2.159(3) Å and [**8a**]$^+$[SbF$_6$]$^-$ [2.150(5) Å] are equal within experimental error and are significantly shorter than that in **8b** [2.179(2) Å].

Voltammetry. Cyclic and alternating current (AC) voltammograms measured either at −60 °C or at room temperature in CH$_2$Cl$_2$ showed that the ruthenium(II) complexes [Ru(acac)$_2$(LL′)] (**8**−**14**) undergo reversible oxidation in the potential range +0.32 to +0.60 V referred to Ag/AgCl. The voltammograms appeared as the superposition of two peaks of different intensities; these were best resolved in AC voltammetry, where the standard response for reversible one-electron transfer is a symmetric peak (ideally of 90 mV width at half-height at 293 K and 70 mV at 233 K, but typically broadened by ohmic

---

(57) Matsuzawa, H.; Ohashi, Y.; Kaizu, Y.; Kobayashi, H. *Inorg. Chem.* **1988**, *27* 2981.

(58) Knowles, T. S.; Howlin, B. J.; Jones, J. R.; Povey, D. C.; Amodio, C. A. *Polyhedron* **1993**, *12*, 2921.

Table 5. Redox Potentials ($E_{1/2}$) (Ru^{III}/Ru^{II}) and Diastereomer Ratios of Isolated Complexes $[Ru(acac)_2(LL')]^{n+}$ ($n = 0$, 1)

	$E_{1/2}{}^{a}$	% at Ru^{II} level	% at Ru^{III} level
8a	+0.42	55 (10)[b]	70
8b	+0.52	45 (90)[b]	30
9a	+0.39	40 (15)[c]	70
9b	+0.47	60 (85)[c]	30
10a	+0.32	40	75
10b	+0.44	60	25
11a	+0.38	40	80
11b	+0.47	60	20
12a	+0.44	5	80
12b	+0.52	95	20
13a	*d*	5	*e*
13b	+0.60	95	*e*
14a	+0.43	5	80
14b	+0.53	95	20

[a] Vs Ag/AgCl at −60 °C. [b] After 72 h at 90 °C in vacuo or heating in refluxing toluene. [c] After 2 h at 70 °C in vacuo or recrystallization. [d] Could not be determined owing to low abundance of **13a** at Ru^{II} level. [e] Not determined.

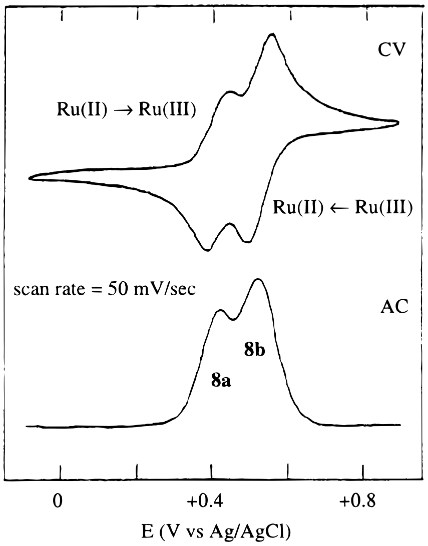

Figure 5. Cyclic and AC voltammograms of $[Ru(acac)_2(o\text{-}CH_2{=}CHC_6H_4NMe_2)]$ containing **8a** (ca. 40%) and **8b** (ca. 60%) in CH_2Cl_2 at −60 °C.

losses).[59] The ratio of the areas of the superimposed voltammograms matched the ratio of **a** and **b** isomers derived from the ^1H NMR spectra; hence, the waves reflect the one-electron oxidation of the **a** and **b** isomers to the corresponding isomers of $[Ru(acac)_2(LL')]^+$ (**8**$^+$−**14**$^+$). As shown in Table 5, the oxidation potentials of the **a** and **b** isomers differ by 80−140 mV, the **a** isomer (which is usually the less abundant) having the lower value of $E_{1/2}$ ($Ru^{3+/2+}$), i.e., being the more easily oxidized. As an example, the cyclic and AC voltammograms of the 2-vinyl-*N,N*-dimethylaniline complex containing **8a** (ca. 40%) and **8b** (ca. 60%) are shown in Figure 5. The corresponding $E_{1/2}$ ($Ru^{3+/2+}$) values, +0.42 and +0.52 V, respectively, were confirmed by voltammetry of the separated isomers and of $[\mathbf{8}]^+[PF_6]^-$ (see below).

Cyclic and AC voltammetry of the isolated ruthenium(III) complexes $[Ru(acac)_2(LL')]^+$ (**8**$^+$−**12**$^+$) in CH_2Cl_2 in the temperature range −60 °C to +20 °C showed the expected reversible one-electron reduction to the parent ruthenium(II) complexes. Again, there were two waves in each voltammogram, corresponding to reduction of the **a**$^+$ and **b**$^+$ isomers at different potentials. However, the relative areas of the superposed voltammograms were different from those observed in the oxidation of **8**−**12**, the peak due to **a**$^+$ now being considerably more intense than that due to **b**$^+$ (ca. 7:3). In contrast to the behavior of mixtures of **8a** and **8b**, the observed ratios did not change when the samples were heated in vacuo at or above room temperature. Clearly, isomerization from **b** to **a** occurs during the formation of the ruthenium(III) cations by chemical oxidation of their ruthenium(II) precursors, the time scale of this process being much slower than that of cyclic voltammetry (seconds). The diastereomers of Figure 2 probably interconvert by reversible ligand dissociation, although one-ended dissociation of acac and a nondissociative trigonal twist mechanism cannot be excluded. These processes clearly do not occur rapidly at the ruthenium(II) level, and in view of the relative weakness of the alkene−ruthenium(III) bond suggested by the structure of $[\mathbf{8a}]^+[SbF_6]^-$, it seems likely that the lability of this bond is responsible for the observed isomerization behavior.

Spectroelectrochemistry. The electronic spectra of the ruthenium(II) complexes **8**−**14** exhibit a broad band consisting of two components in the range 25 000−33 000 cm^{-1}, which probably arise largely from charge-transfer transitions within the *cis*-Ru(acac)$_2$ fragment, and a stronger absorption near 37 000 cm^{-1}, which is probably the $\pi \rightarrow \pi^*$ transition characteristic of acac$^-$ and its complexes. For example, in the case of the 2-vinyl-*N,N*-dimethylaniline complex **8** (**8a**, 45%; **8b**, 55%), there are two broad features in the range 22 000−33 000 cm^{-1} ($\epsilon = 3600$ and 5500 M^{-1} cm^{-1}, respectively) and an absorption at 37 000 cm^{-1} ($\epsilon = 14\,100$ M^{-1} cm^{-1}). This spectrum is the expected superposition of the spectra of the separate isomers, which differ appreciably. For **8a** there is one distinct broad band at 26 500 cm^{-1} and a second broad band at ca. 30 000 cm^{-1} that overlaps an intense absorption with a maximum at 36 300 cm^{-1}; for **8b** there are two overlapping broad bands with maxima at ca. 27 300 cm^{-1} and 31 100 cm^{-1}, and an intense absorption at 37 400 cm^{-1}.

The electronic spectra of the ruthenium(III) complexes **8**$^+$−**12**$^+$ consist of two broad bands with maxima at 15 300−17 200 cm^{-1} and 33 700−35 200 cm^{-1}, e.g., for **8**$^+$ (**8a**$^+$, 70%; **8b**$^+$, 30%) the bands are at 16 300 cm^{-1} ($\epsilon = 2100$ M^{-1} cm^{-1}) and 33 900 cm^{-1} ($\epsilon = 9500$ M^{-1} cm^{-1}). The lower energy band is assigned tentatively to an acac (π) → Ru(III) (LMCT) transition, the higher energy band to an acac ($\pi \rightarrow \pi^*$) transition. The experiments described below showed that the electronic spectra of pure **8a**$^+$ and **8b**$^+$ do not differ.

We have used spectroelectrochemistry to explore the course of the isomerization of the ruthenium(III) complexes at various temperatures by performing electrooxidation or electroreduction in an optically transparent thin-layer (OTTLE) cell. Figure 6 shows a set of optical spectra generated by one-electron oxidation at −60 °C of a 40:60 mixture of **8a** and **8b** at an applied potential of +0.8 V vs Ag/AgCl (i.e., about 300 mV greater than the $E_{1/2}$-value for the less easily oxidized isomer **8b**). The trace is clearly the superposition of two sets of spectra. The spectra of the first set, (**a**), generated in the first phase of the electrolysis, intersect in isosbestic points at 22 100, 30 700, 34 800 and 41 200 cm^{-1}; these arise from bulk oxidation of the more easily oxidizable isomer **8a** ($E_{1/2} = +0.42$ V) to **8a**$^+$. Although both **8a** and **8b** are undoubtedly oxidized at the electrode, diffusion-limited homogeneous cross-reaction of **8b**$^+$ with residual **8a** ensures that bulk oxidation of **8a** is accomplished first. This process is accompanied by a loss of intensity in the band near 37 000 cm^{-1}. When this oxidation is complete, a second spectral progression appears, which is

---

(59) Smith, D. E. *Electroanal. Chem.* **1966**, *1*, 1.

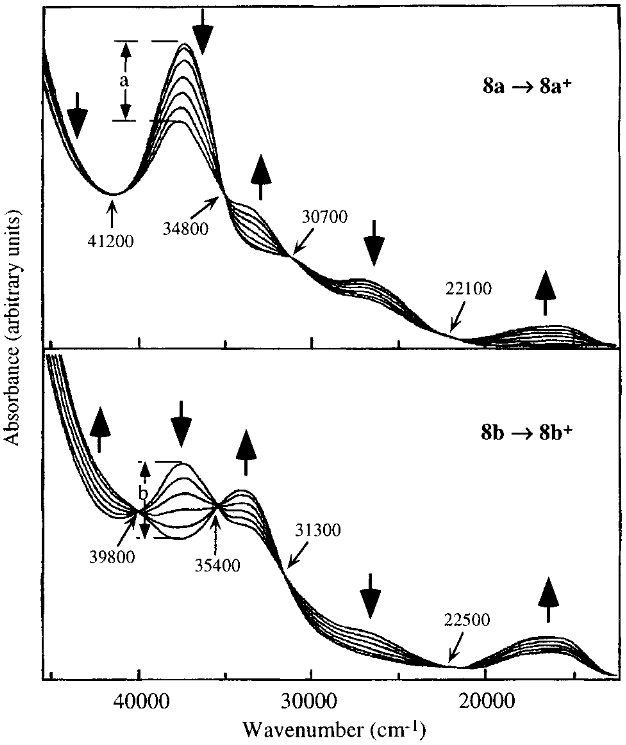

Figure 6. Electronic spectra recorded during one-electron oxidation of [Ru(acac)$_2$(*o*-CH$_2$=CHC$_6$H$_4$NMe$_2$)] containing **8a** (ca. 40%) and **8b** (ca. 60%) in CH$_2$Cl$_2$ at −60 °C.

characterized by a different set, **b**, of isosbestic points at 22 500, 31 300, 35 400, and 39 800 cm^{-1}; these arise from exclusive oxidation of the less easily oxidizable isomer **8b** ($E_{1/2} = +0.52$ V). With the removal of **8b**, the band at 37 000 cm^{-1} collapses completely (Figure 6). The ratio of the successive reductions of intensity equals the ratio of **8a** to **8b** in the initial ruthenium(II) complex, the spectrum of which is regenerated when the mixture of **8a**$^+$ and **8b**$^+$ is electroreduced ($E_{\mathrm{appl}} = +0.1$ V).

As expected, similar processes occurred in the opposite order when a sample of [**8**]PF$_6$ [**8a**$^+$, 70%; **8b**$^+$, 30%] was reduced at −60 °C ($E_{\mathrm{appl}} = +0.1$ V). In this case, the increase in intensity of the band near 37 000 cm^{-1} in the first phase corresponds to the formation of **8b**, in the second phase to the formation of **8a**, and the ratio of the increases agrees well with the initial ratio of **8a**$^+$ to **8b**$^+$. Subsequent electrooxidation ($E_{\mathrm{appl}} = +0.8$ V) regenerated the initial mixture of **8a**$^+$ and **8b**$^+$. The results were confirmed by carrying out similar experiments on pure **8b** and **8a**$^+$. Thus the redox processes **8a** $\rightleftarrows$ **8a**$^+$ and **8b** $\rightleftarrows$ **8b**$^+$ are fully reversible at −60 °C.

The process of chemical oxidation was modeled by a spectroelectrochemical experiment in which the 40:60 mixture of **8a** and **8b** was oxidized at room temperature ($E_{\mathrm{appl}} = +0.8$ V) to the corresponding mixture of **8a**$^+$ and **8b**$^+$ and set aside at this potential for a fixed period at room temperature. The solution was then cooled to −60 °C in order to freeze out any isomerization processes and reduced back to **8a**/**8b**. The electronic spectra showed the proportions of **8a**:**8b** in this solution to be 60:40 after 3 h and ca. 85:15 after 11 h, corresponding to the proportions of **8a**$^+$ and **8b**$^+$ in the original oxidized solution. Independent experiments showed that **8b**$^+$, electrogenerated similarly from pure **8b**, is thermally stable only between −60° and −10 °C. Above −10 °C, **8b**$^+$ isomerizes to **8a**$^+$; at room temperature, the proportions of **8a**$^+$ in a solution of **8b**$^+$ rose from ca. 60% after 3 h to a limiting value of ca. 85%.

Discussion

Among the d-block elements, monomeric ruthenium(II) and osmium(II) ions bearing purely σ-donor ligands such as H$_2$O and NH$_3$ show an ability to bind unsaturated ligands that is unrivaled among classical coordination compounds. This behavior has been attributed to the π-back-bonding ability of the nd^6 metal center.[60] The stability of the [Ru(acac)$_2$(LL′)] complexes **8**−**14** is a further indication of this property. However, the presence of the anionic β-diketonate ligands shifts the redox potentials in favor of the higher oxidation state, thus enabling for the first time the isolation of the ruthenium(III) (4d^5) counterparts, [Ru(acac)$_2$(LL′)]$^+$ (**8**$^+$−**12**$^+$, **14**$^+$). So far as we are aware, these pairs represent the only isolable mononuclear monoalkene complexes of any transition element having the same basic structure but differing only in the oxidation state of the metal atom; however, the binuclear μ-octamethylcyclooctatetraene pair [Mo$_2$(η^5-C$_5$H$_5$)$_2$(μ-C$_8$Me$_8$)]$^{n+}$ ($n = 0, 1$) has been studied and structurally characterized.[61] A limited number of mononuclear 18-electron/17-electron pairs is known for alkyne complexes, e.g., [Os(NH$_3$)$_5$(η^2-PhC$_2$Ph)]$^{n+}$ ($n = 2,3$),[62] [Cr(CO)$_2$(η^2-PhC$_2$Ph)(η^6-C$_6$HMe$_5$)]$^{n+}$ ($n = 0, 1$),[63] and[Mo(CO)$_2$(η^2-PhC$_2$Ph)(Tp′)]$^{n+}$ ($n = 0, 1$) [Tp′ = HB(3,5-dimethylpyrazolyl)$_3$],[63] and for molybdenum complexes containing η^3-allyl and η^4-diene ligands, [Mo(η^5-C$_5$H$_5$)(η^3-C$_3$H$_5$)(η^4-C$_4$H$_6$)]$^{n+}$ ($n = 0, 1$).[64] Comparison of the Ru−C and C=C bond lengths of **8a** and **8b** with those in **8a**$^+$ indicates weaker binding of the alkene in **8a**$^+$. On the basis of the Dewar−Chatt−Duncanson model, the electron removed on oxidation resides in a HOMO arising from overlap of a filled metal orbital (t$_{2g}$ in a regular octahedron) with an alkene π*-orbital; thus, in agreement with earlier suggestions,[60] π-back-bonding is probably reduced at the ruthenium(III) level, but not enough to prevent alkene coordination. A similar trend in M−C and C=C distances is observed for the metal−alkene distances involving one of the molybdenum atoms in the pair [Mo$_2$(η^5-C$_5$H$_5$)$_2$(μ-C$_8$Me$_8$)]$^{n+}$ ($n = 0, 1$), and a similar explanation to that given above has been advanced.[61] In contrast, the metal−carbon bonds of the alkyne complexes [Cr(CO)$_2$(η^2-PhC$_2$Ph)(η^6-C$_6$HMe$_5$)],[63] [Mo(CO)$_2$(η^2-PhC$_2$Ph)(Tp′)],[63] and [Ru(acac)$_2$(η^2-*o*-PhC$_2$C$_6$H$_4$NMe$_2$)][65] are shortened, and presumably strengthened, as a consequence of one-electron oxidation, because the electron is removed from an antibonding orbital derived from the filled $\pi_\perp$ orbital of the alkyne.

We have established that the bis(acetylacetonato) complexes of Ru(II) (4d^6) and Ru(III) (4d^5) have opposite preferences for enantioface coordination of 2-vinyl-*N*,*N*-dimethylaniline (**1**), the ratio of *R*Δ/*S*Λ (**a**) to *S*Δ/*R*Λ (**b**) diastereomers at equilibrium being ca. 1:9 for Ru(II) and ca. 6:1 for Ru(III). The complexes of the other chelate ligands, **2**−**7**, seem to behave similarly. In view of the rather small differences in metal−ligand distances between **8a**, **8b**, and [**8a**]$^+$, we suggest that an electronic effect associated with maximizing interaction of the alkene π*-orbital with a filled metal d-orbital may be responsible for this behavior. It is interesting that a similar difference of orientation is observed

---

[60] (a) Taube, H. *Pure Appl. Chem.* **1979**, *51*, 901; **1991**, *63*, 651. (b) Taube, H. *Comments Inorg. Chem.* **1981**, *1*, 17.

[61] Connelly, N. G.; Metz, B.; Orpen, A. G.; Rieger, P. H. *Organometallics* **1996**, *15*, 729.

[62] Harman, W. D.; Wishart, J. F.; Taube, H. *Inorg. Chem.* **1989**, *28*, 2411.

[63] Bartlett, I. M.; Connelly, N. G.; Orpen, A. G.; Quayle, M. J.; Rankin, J. C. *Chem. Commun.* **1996**, 2583.

[64] Wang, L.-S.; Fettinger, J. C.; Poli, R. *J. Am. Chem. Soc.* **1997**, *119*, 4453.

[65] Bennett, M. A.; Heath, G. A.; Kovacik, I.; Willis, A. C. unpublished work.

in the molybdenum complexes Mo(η^5-C_5H_5)(η^3-C_3H_5)(η^4-C_4H_6)]$^{n+}$ (n = 0,1): the allyl group in the major isomer at the Mo(II) level is in the "prone" position, whereas at the Mo(III) level it is "supine".[64]

In the case of the N-donor complexes of ruthenium(II) **8**, **10**, and **11** containing coordinated $CH{=}CH_2$, the diastereomeric equilibrium is reached only slowly, the final ratio of **a** to **b** of ca. 1:9 being established only after several days at ca. 100 °C. One-ended dissociation, either of the acac ligands or of the unsaturated chelate group, evidently does not occur readily. In contrast, complex **9** containing coordinated $C(CH_3){=}CH_2$ isomerizes within a few hours at 70 °C to the equilibrium ratio of diastereomers, possibly reflecting steric destabilization by the alkene methyl group of the metal−alkene interaction. Complexes **12**−**14** appear to contain the thermodynamic diastereomeric ratio (ca. 1:9) immediately after isolation, presumably because the generally poorer ligating ability of O-donors relative to that of their N-donor counterparts allows more ready dissociation of the alkene from the coordination sphere.

Finally, and more speculatively, the dependence of the preferred orientation of a coordinated prochiral alkene on metal d-electron count could play a role in catalytic processes involving the insertion of alkenes into metal−carbon bonds. A notable example is the different behavior toward propylene of catalysts based on titanium(III) ($3d^1$) and vanadium(III) ($3d^2$): the former tend to give isotactic polypropylene, whereas the latter favor the syndiotactic form.[66,67]

Acknowledgment. We thank Mr. Horst Neumann for experimental assistance and for the synthesis of [Ru(acac)$_2$($CH_2{=}CHCH_2CH_2OCH_3$)]PF_6 (**14**).

Supporting Information Available: Crystallographic data, atomic coordinates and isotropic displacement parameters, anisotropic displacement parameters, interatomic distances and angles for hydrogen and non-hydrogen atoms, torsion angles for non-hydrogen atoms, and selected least-squares planes for **8a**, **8b**, and [**8a**]$^+$[SbF_6]$^-$ (62 pages). See any current masthead page for ordering and Internet access instructions.

JA973282K

---

[66] Yamamoto, A. *Organotransition Metal Chemistry: Fundamental Concepts and Applications*; Wiley: New York, 1986; pp 312−315.

[67] Suzuki, T.; Takegami, Y. *Bull. Chem. Soc. Jpn.* **1970**, *43*, 1484.